ACS Medicinal Chemistry Letters

pubs.acs.org/acsmedchemlett

Letter

Balancing Nonsense Mutation Readthrough and Toxicity of Designer Aminoglycosides for Treatment of Genetic Diseases

Sandip Guchhait,[†] Alina Khononov,[†] Tomasz Pieńko,[†] Valery Belakhov, and Timor Baasov*

Cite This: *ACS Med. Chem. Lett.* 2023, 14, 794−801

Read Online

ACCESS | Metrics & More | Article Recommendations | Supporting Information

ABSTRACT: New derivatives of aminoglycosides with a side chain 1,2-aminoalcohol at the 5" position of ring III were designed, synthesized, and biologically evaluated. The novel lead structure (compound **6**), exhibiting substantially enhanced selectivity toward eukaryotic versus prokaryotic ribosome, high readthrough activity, and considerably lower toxicity than the previous lead compounds, was discovered. Balanced readthrough activity and toxicity of **6** were demonstrated in three different nonsense DNA-constructs underlying the genetic diseases, cystic fibrosis and Usher syndrome, and in two different cell lines, baby hamster kidney and human embryonic kidney cells. Molecular dynamics simulations within the A site of the 80S yeast ribosome demonstrated a remarkable kinetic stability of **6**, which potentially determines its high readthrough activity.

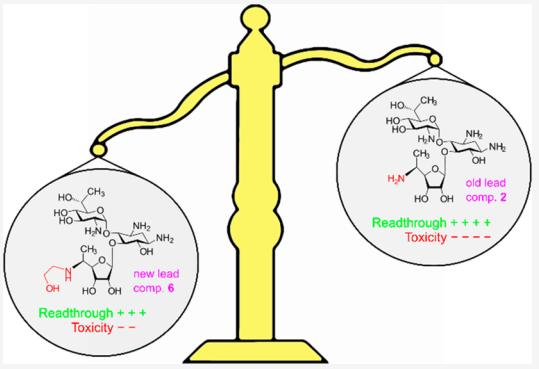

KEYWORDS: *Aminoglycosides, genetic diseases, nonsense mutations, translational readthrough, cystic fibrosis*

Nonsense mutations account for about 10−12% of all inherited human diseases including cystic fibrosis (CF), Duchenne muscular dystrophy (DMD), Usher syndrome (USH), Hurler syndrome (HS), and a variety of cancers.[1] These mutations are genetic code mutations usually occurring due to base pair insertions, deletions, or substitutions that produce the premature termination codon (PTC) by replacement of an amino-acid coding codon in DNA with one of the three universal stop codons (TAA, TGA, or TAG). These mutations lead to production of truncated and nonfunctional proteins, which results in disease.[2] Curative therapies do not exist for most nonsense mutation diseases, and the only treatment widely used is symptomatic.

One approach to the treatment of these diseases is the use of small molecules that induce the ribosome to selectively readthrough the PTC signal but not the natural stop signal in the mutant mRNA, and thereby allow the production of full-length functional protein.[3] This therapeutic strategy, also called "PTC suppression therapy" or "translational readthrough", was first demonstrated by using certain structures of aminoglycoside antibiotics like gentamicin and G418. A series of *in vitro* and *in vivo* studies that included clinical trials clearly highlighted the potential of aminoglycosides as promising therapeutics for treatment of genetic diseases caused by PTCs.[4−6] Unfortunately, conventional aminoglycosides exhibiting readthrough activity are also toxic to mammals, which in turn limited their clinical benefit for PTC suppression therapy.

To address these issues, in recent years, our lab has systematically modified conventional aminoglycosides and developed new lead compounds of NB series (e.g., compounds **1** and **2**, also named NB74 and NB124, respectively, Figure 1) with improved readthrough activity and reduced toxicity as demonstrated in various models of different diseases caused by PTC mutations.[7−10] One of these derivatives, compound **2** (NB124 or ELX-02), is currently in Phase 2 clinical trials for treatment of CF.[11−13] The reduced toxicity of **1** and **2** and of other developed leads in comparison to the conventional aminoglycosides like gentamicin and G418 was attributed to their significantly enhanced selectivity toward the mammalian cytoplasmic ribosome along with reduced selectivity toward the mitochondrial ribosome.[12,14] These studies provided the proof of principle that by using chemical tools, antibacterial activity and toxicity of aminoglycoside antibiotics can be dissected from their PTC readthrough activity. Specifically, it was shown that the increased specificity toward eukaryotic cytoplasmic ribosome correlates with the increased PTC suppression activity and that the decreased specificity toward mitochondrial ribosome confers the lower toxicity.

Despite these considerable pharmacodynamic gains, the clinical toxicity profile of the designer aminoglycoside remains the central issue and research focus for its further development as a PTC readthrough agent for treatment of genetic diseases.

Received: March 9, 2023
Accepted: April 17, 2023
Published: April 27, 2023

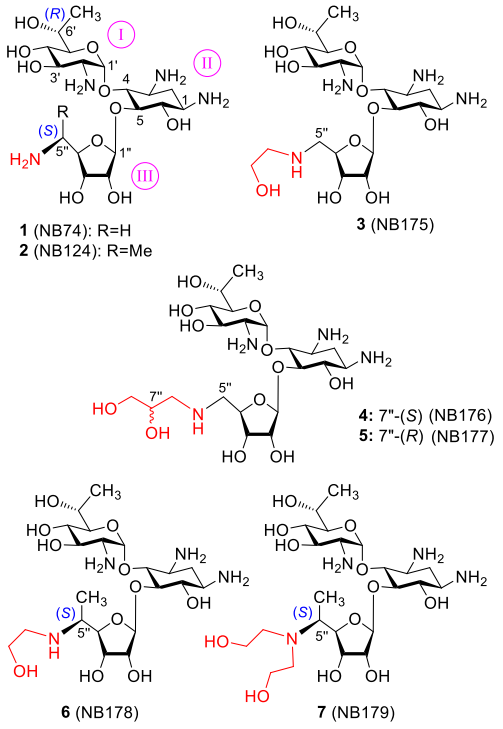

Figure 1. Chemical structures of synthetic AGs that were investigated in this study.

Indeed, PTC Therapeutics recently reported on the synthesis and biological tests of a large library of new derivatives of G418,[15] since it has long been known as the most active readthrough inducer[16] but also as one of the most toxic aminoglycosides.[17] However, unfortunately this work did not identify a novel aminoglycoside derivative which improved upon G418. More recently, Powell and colleagues have reported on their efforts to reduce toxicity but maintain PTC readthrough activity of the previously reported designer aminoglycosides by reducing their overall cationic charge.[18] Specifically, they chose to modify compound NB124[12] (**2**, Figure 1) and compound NB157[19] (a compound like **2** but with an additional hydroxyl at 6′-methyl) by replacing the 2′-amine of ring I with a hydroxyl group. The corresponding 2'-OH variants were further evaluated for their PTC readthrough activity and cytotoxicity, and as expected, the resulted structures exhibited relatively lower cytotoxicity than their parent structures did. However, this reduction in cytotoxicity of the designer 2'-OH derivatives was accompanied by a significant reduction (>10-fold) in their PTC suppression activity. These observations prompted us to ask: is it possible to significantly reduce the toxicity of the designer aminoglycosides without detrimentally impacting their readthrough activity?

To address this question, herein we report on the design, synthesis, and evaluation of the new pseudotrisaccharides **3**−**7** (Figure 1) that differ from our previous leads **1** and **2** by the presence of an 1,2-aminoalcohol at the 5" position of ring III. We discovered the new lead structure, compound **6**, that exhibits high readthrough activity and substantially lower toxicity than the previous lead, compound **2**.

In selecting the 5" position as the modification site in **1** and **2**, we have taken into consideration the following points. First, our recently solved 3D structures of the aminoglycoside paromomycin in Leishmania ribosomal A-site elucidated the superiority of the 5″-NH_2 moiety in all our previously reported NB-compounds over the 5"-OH in the standard 4,5-disubstituted aminoglycosides (e.g., paromomycin) for enhanced binding and selective action of NB-compounds toward eukaryotic versus prokaryotic ribosomes.[20,21] Second, the reduced basicity of particular amines in the aminoglycoside structure has been directly correlated to decreased toxicity.[22] For example, installation of the electron-withdrawing 3′-OH in tobramycin renders the 2′-amino group less basic and results in a significantly less toxic aminoglycoside kanamycin B.[23] Similarly, replacement of the 5-OH with 5-fluorine in kanamycin B and its clinical variants gave significantly fewer toxic derivatives.[24,25] Based on these data, we reasoned that (i) the installation of an ethyl-alcohol moiety directly on the 5″-NH_2 of **1** and **2** would significantly reduce the basicity of the 5″-amino group in the resulting new derivatives **3**−**6** (5″-NH_2 → 5″-NH−CH_2CH_2−OH), and (ii) thereby confer reduced toxicity for **3**−**6**. Compound **7** consists of two such ethyl-alcohol appendages and is a tertiary 5″-amine. Compounds **3**−**5** are new derivatives of our previously reported lead compound **1**,[10] while compounds **6** and **7** are derivatives of lead compound **2**.[12]

For the synthesis of **3**−**5**, we employed the common donor intermediate **11** which was readily accessible from the known thioglycoside **8**[7] as shown in Scheme 1. Selective protection of

Scheme 1[a]

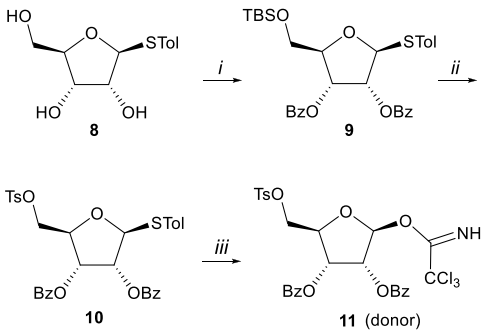

[a]Reagents and conditions: (i) (a) TBSCl, Py, 0−25 °C, 92%, (b) BzCl, Py, DMAP, 0−25 °C, 88%; (ii) (a) TBAF, 0−25 °C, 7 h, 79%; (b) TsCl, Py, DMAP, 0−25 °C, 74%; (iii) (a) NBS, Acetone:H_2O [9:1], −30 °C; (b) CCl_3CN, DBU, CH_2Cl_2, 0 °C, 94% over 2 steps.

the primary hydroxyl as the TBS ether was followed by benzoylation of the remaining hydroxyls to afford **9**. Next, the TBS group was removed with TBAF, and the resulting alcohol was tosylated to obtain **10**. Hydrolysis of the anomeric thioglycoside with NBS in aqueous acetone, and subsequent treatment of the resulting hemiacetals with CCl_3CN/DBU furnished the donor **11** in good yields, which was used in glycosylation reactions without further purification.

The common intermediate **13** was obtained in two chemical steps: coupling of the donor **11** with the known acceptor **12**[10] (BF_3·Et_2O, Scheme 2), followed by hydrolysis of all the ester protections by treatment with $MeNH_2$ (68% yield over 2 steps). Separate treatment of **13** with 2-aminoethanol, (*S*)-3-aminopropane-1,2-diol, or (*R*)-3-aminopropane-1,2-diol in MeOH/H_2O (1:1) under reflux gave the corresponding substituted products, which after Staudinger reaction afforded the target pseudotrisaccharides **3**−**5**.

https://doi.org/10.1021/acsmedchemlett.3c00089
ACS Med. Chem. Lett. 2023, 14, 794−801

Scheme 2[a]

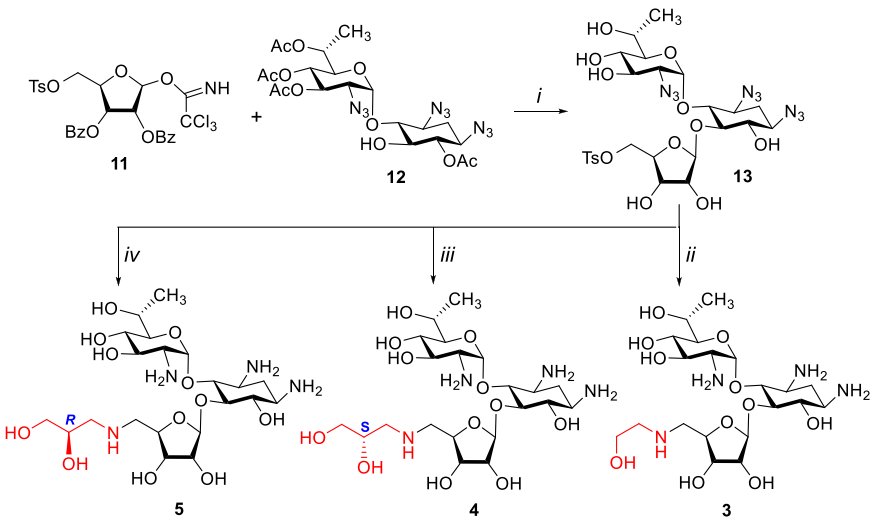

[a]Reagents and conditions: (i) (a) $BF_3{\cdot}Et_2O$, dry CH_2Cl_2, −30 °C; (b) $MeNH_2$ (33% in EtOH), 25 °C, 68% after 2 steps; (ii) (a) $HOCH_2CH_2NH_2$, MeOH/H_2O(1:1), 80 °C, 86%; (b) PMe_3, NaOH (0.1 M), THF, 25 °C, 53%; (iii) (a) (*S*)-3-aminopropane-1,2-diol, MeOH/H_2O(1:1), 80 °C, 71%; (b) PMe_3, NaOH (0.1 M), THF, 25 °C, 53%; (iv) (a) (*R*)-3-aminopropane-1,2-diol, MeOH/H_2O(1:1), 80 °C, 76%; (b) PMe_3, NaOH (0.1 M), THF, 25 °C, 64%.

For the synthesis of **6** and **7**, we designed and constructed the donor **17** as illustrated in Scheme 3. The known

Scheme 3[a]

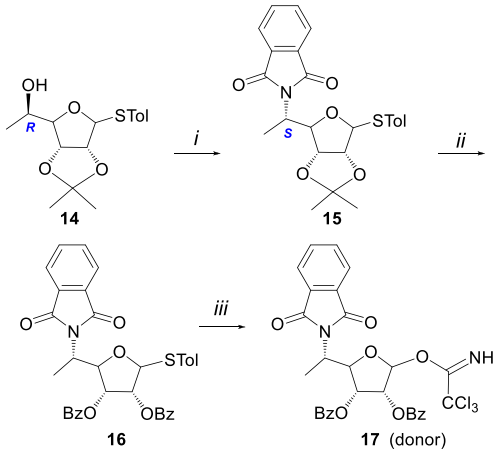

[a]Reagents and conditions: (i) DEAD, PPh_3, phthalimide, THF, 0-25 °C, 86%; (ii) (a) CSA, MeOH/CH_2Cl_2 (1:1), 40 °C, 90%; (b) Py, BzCl, DMAP, 0-25 °C, 98%; (iii) (a) NBS, Acetone/H_2O(9:1), −30 °C; (b) CCl_3CN, DBU, CH_2Cl_2, 0 °C, 94% after 2 steps.

thioglycoside **14**[11] was first converted to its phthalimide derivative **15** with inverted configuration at the side-chain carbon by using Mitsunobu reaction (PPh_3/DEAD). Next, the familiar two-step conversion of the anomeric thioglycoside to the corresponding trichloroacetimidate (shown above in Scheme 1) provided the target donor **17** (94% yield over 2 steps), which was used without purification.

The final steps for the assembly of **6** and **7** are illustrated in Scheme 4. Glycosylation of the acceptor **12**[10] with donor **17** ($BF_3.Et_2O$) furnished the protected coupled product **18** in 89% isolated yield. Next, all the ester and phthalimide protections were removed by treatment with $MeNH_2$ (33% in EtOH) to obtain free primary amine **19**.

Treatment with 2-bromoethanol (1.5 equiv, Cs_2CO_3/CH_3CN) at 70 °C for 24 h gave the major monosubstituted product (secondary amine product) and minor quantities of the disubstituted product (tertiary amine product), which could be separated by column chromatography. However, using 4 equiv of 2-bromoethanol and extension of the reaction for 60 h, gave complete conversion of the starting material (primary amine **19**) to the disubstituted product (tertiary amine). Staudinger reaction of each of the mono- and disubstituted products was performed separately to furnish **6** and **7**, respectively.

The new structures **3**−**7** were initially tested for their comparative *in vitro* PTC suppression efficacy using the parent leads **1** and **2** as standards (Figure 2). These tests in a R3X construct, representing Usher-1 (USH) syndrome,[9] clearly showed that compounds **3** and **6** exhibit significantly enhanced activity in comparison to the lead **1**. Compounds **4**, **5**, and **7**, however, exhibited poorer readthrough activity than **1**, possibly due to the increased steric hindrance in these compounds that is induced by the extended side chain at the 5″ position in **4** and **5**, and the two CH_2CH_2OH groups at 5″-nitrogen in **7**.

The observed reduction in PTC suppression activity of **4**, **5**, and **7** was further supported by their significantly reduced inhibition of eukaryotic protein translation (Table 1). The measured half-maximal inhibitory concentration values, IC_{50}^{Euk}, for **4**, **5**, and **7** are 2.5-, 6.9-, and 4-fold higher compared to that of compound **1** (IC_{50}^{Euk} values of 29.5, 81.9, 47.2, and 11.8 μM, respectively). In contrast, two other new compounds **3** and **6** that displayed significantly better readthrough than **1** both have similar IC_{50}^{Euk} values (12.7 and 11.1 μM, respectively) to that of compound **1** (11.8 μM). This observation was rather unexpected since in our previous studies we regularly observed a correlation between IC_{50}^{Euk} and readthrough: increased specificity toward the eukaryotic ribosome (reduced IC_{50}^{Euk}) associated with increased readthrough.[12,20] Indeed, the lead **2**, that displayed the highest readthrough (Figure 2), was also the

https://doi.org/10.1021/acsmedchemlett.3c00089
ACS Med. Chem. Lett. 2023, 14, 794−801

Scheme 4[a]

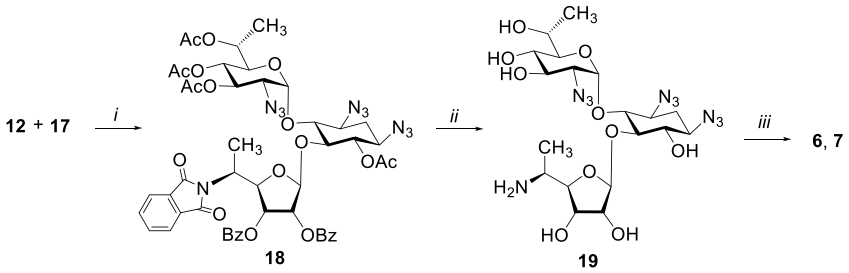

[a]Reagents and conditions. (i) $BF_3{\cdot}Et_2O$, dry CH_2Cl_2, −30 °C, 89%; (ii) $MeNH_2$ (33% in EtOH), 25 °C, 83%; (iii) (a) Cs_2CO_3, $HOCH_2CH_2Br$, CH_3CN, 70 °C, (b) PMe_3, NaOH (0.1 M), THF, 0-25 °C, 27% of **6** after 2 steps, 37% of **7** after 2 steps.

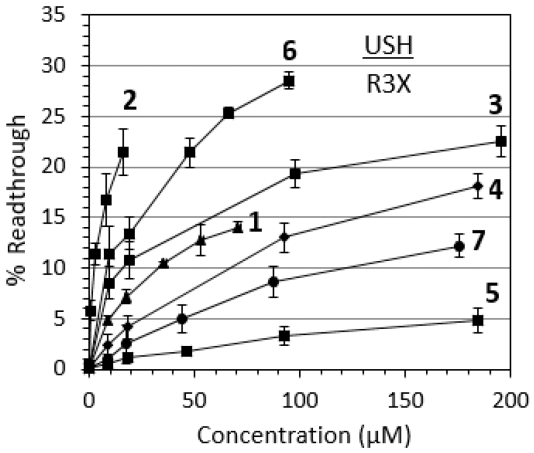

Figure 2. Comparative *in vitro* stop codon suppression levels induced by compounds **1**−**7** in R3X construct, representing Usher-1 syndrome. The assays were performed as previously described by us.[12] The results are averages of at least three independent experiments.

strongest inhibitor (the smallest IC_{50}^{Euk} value, 1.7 μM, Table 1). With the new compounds **3** and **6**, however, such a correlation is broken: the readthrough ranks as **6** > **3** > **1**, while all three have similar IC_{50}^{Euk} values. Further discussion on this issue is given below in the molecular dynamics simulations section.

We have previously demonstrated that the decreased prokaryotic ribosome specificity of **1** and **2** is linked to their reduced mitochondrial translation inhibition and consequently to their reduced cytotoxic and ototoxic effects compared to those for gentamicin and G418.[12,14] We therefore tested the comparative impacts of **1**−**7** in prokaryotic system as well using the gentamicin and G418 as standards.

The measured IC_{50}^{Pro} values (Table 1) show that the efficacy with which compound **6** inhibits the prokaryotic ribosome is like that of the parent compounds **1** and **2** (IC_{50}^{Pro} values of 1.02, 0.85, and 1.66 μM, respectively) and are far lower than that of gentamicin and G418 (IC_{50}^{Pro} values of 0.028 and 0.09 μM, respectively). Thus, **6**, **1**, and **2** exhibit a similar impact on the bacterial ribosome, which suggests that **6** might exhibit reduced cytotoxicity and ototoxicity potential.

As expected, the measured comparative IC_{50}^{Pro} values generally agree with the observed antibacterial data of this set of compounds (Table 1). Thus, while gentamicin and G418 exhibit excellent antibacterial activities against both Gram-negative *Escherichia coli* (R477−100) and Gram-positive *Bacillus subtilis* (ATCC-6633), all the designer compounds **1**−**7** lack significant antibacterial activity. The data with **3**−**7** is like that observed for **1** and **2** and further supports the previously reported correlation in aminoglycosides between prokaryotic anti translational activity and MIC values: decreased inhibition of prokaryotic translation is associated with the decrease in antibacterial activity.

Table 1. Comparative Inhibition of Translation in Eukaryotic and Prokaryotic Systems, Cytotoxicity, and Antibacterial Activity

	translation inhibition[a]			cell toxicity LC_{50} (mM)[b]		antibacterial activity MIC (μg/mL)[c]	
compd	IC_{50}^{Euk} (μM)	IC_{50}^{Pro} (μM)	$IC_{50}^{Euk}/IC_{50}^{Pro}$	BHK	HEK293-FT	*E. coli* R477/100	*B. subtilis* ATCC6633
G418	2.0	0.009	222	0.9	1.7	9	1.25
gentamicin	62.0	0.028	2214	1.9	3.6	6	0.75
1	11.8	0.85	13.9	11.4	24.8	>192	48
2	1.7	1.66	1.02	4	7.9	>192	96
3	*12.7*	*0.3*	*42.3*	*2.5*	*3.9*	*96*	*24*
4	29.5	1.5	19.7	n.d	n.d	>192	192
5	81.9	4	20.5	n.d	n.d	>192	>192
6	*11.1*	*1.02*	*10.9*	*12.1*	*19.2*	*>192*	*192*
7	47.2	3.1	15.2	n.d	n.d	>192	>192

[a]The eukaryotic and prokaryotic half-maximal-inhibition values (IC_{50}^{Euk} and IC_{50}^{Pro}) were quantified in coupled transcription/translation assays by using active luciferase detection as previously described by us.[12] The IC_{50}^{Euk} and IC_{50}^{Pro} values were obtained from fitting concentration response curves to the data of at least three independent experiments, using GraFit 5 software. [b]Aminoglycosides-induced cell toxicity was measured in baby hamster kidney (BHK) and human embryonic kidney (HEK293-FT) cells and calculated as a ratio between the number of living cells in cultures grown with and without the presence of the tested compound. [c]The MIC values were determined by using the double-microdilution method, with 192 μg/mL as starting concentration of each tested compound. All the experiments were performed in duplicates and analogous results were obtained in three independent experiments.

https://doi.org/10.1021/acsmedchemlett.3c00089
ACS Med. Chem. Lett. 2023, 14, 794−801

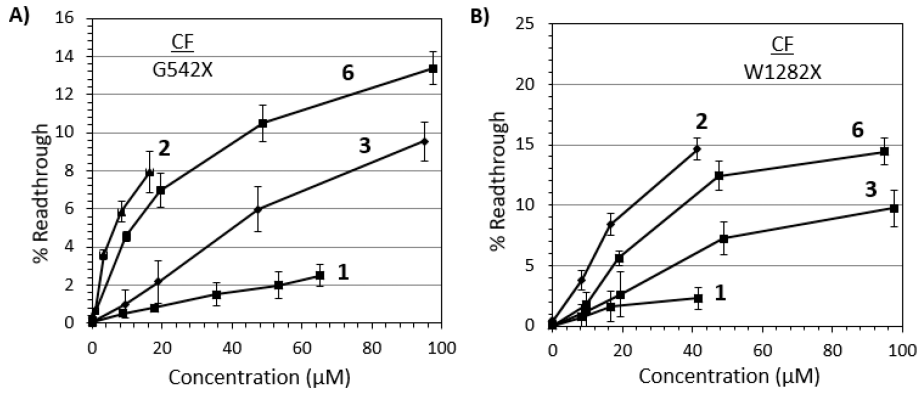

Figure 3. Comparative *in vitro* stop codon suppression level induced by compounds **1**, **2**, **3**, and **6** in two different nonsense constructs, G542X and W1282X, representing cystic fibrosis. The assays were performed as previously described by us.[12] The results are averages of at least three independent experiments.

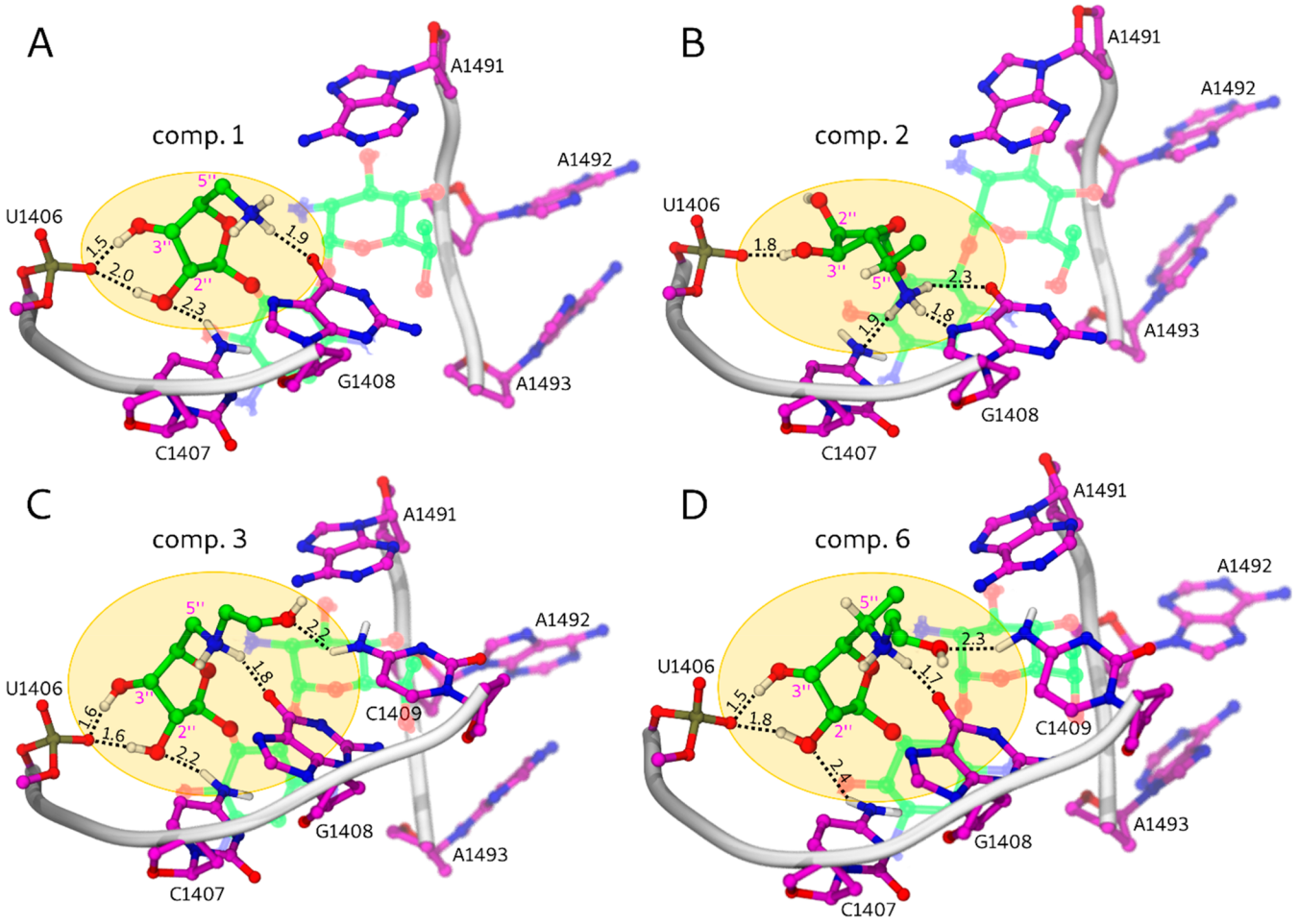

Figure 4. Binding modes of compounds **1**, **2**, **3**, and **6** in the A site of eukaryotic ribosome. For clarity, only the interactions involving ring III (in dark green and highlighted with yellow background) are shown. rRNA nucleotides are numbered according to the *E. coli* numbering. Hydrogen bonds and salt bridges are presented as black dashed lines and bond lengths are in Å.

The readthrough efficiency induced by aminoglycosides is highly dependent on the identity of a stop codon and the sequence context around the stop codon.[16] Therefore, to further evaluate the potential of **3** and **6**, in addition to R3X plasmid (UGA C, Figure 2), we tested two other dual-luciferase reporter plasmids previously developed by us.[9] These plasmids, G542X (UGA G) and W1282X (UGA A), contain different sequence contexts around premature stop codons derived from the CFTR gene. We were pleased to discover that, like the data with R3X, the readthrough activities of both **3** and **6** were significantly enhanced (in comparison to **1**) in G542X and W1282X as well (Figure 3). The data observed in all three plasmids tested clearly substantiate the trend of readthrough potency: **2** > **6** > **3** > **1**. Thus, the activity gap between **1** and **2** is now filled by two new structures, **3** and **6** (see Figures 2 and 3).

https://doi.org/10.1021/acsmedchemlett.3c00089
ACS Med. Chem. Lett. 2023, 14, 794−801

Note that **2** is the main lead compound in clinical trials, and **1** has low readthrough activity but exhibits the lowest cytotoxicity and ototoxicity measured among all our developed NBs.[14,21] To gain a better understanding on the safety of **3** and **6**, we determined their comparative cell toxicity to those of **1** and **2** by measuring the half-maximal lethal concentration values (LC_{50}) in baby hamster kidney (BHK) and in human embryonic kidney (HEK293-FT) cells, using gentamicin and G418 as standards (Table 1).

Among the synthetic derivatives tested, compound **3** is the most cytotoxic (LC_{50} values of 2.5 and 3.9 mM in BHK and HEK293-FT cells, respectively) and is almost as toxic as the clinical drug gentamicin (LC_{50} of 1.9 and 3.6 mM in BHK and HEK293-FT). G418, one of the most cytotoxic aminoglycosides known, exhibited the lowest LC_{50} values in both cell types (0.9 and 1.7 mM, respectively). Interestingly, compound **6** that exhibited the highest readthrough activity among the new derivatives, also showed significantly low toxicity and was as cytotoxic as the compound **1** (LC_{50} values of 12.1 and 11.4 mM in BHK cells, and 19.2 and 24.8 mM in HEK293-FT cells, for **6** and **1**, respectively). Moreover, **6** was about 3- and 2.4-fold less cytotoxic in both cell lines, and only 1.3−1.7 times less active in all three plasmids tested than the lead **2**. The observed comparative cytotoxicity and readthrough activity data identifies the compound **6** as the new lead compound worthy of further drug development.

The observed reduced cytotoxicity of **6** in comparison to **3** stands in correlation with their measured IC_{50}^{Pro} values. Thus, compound **6** that inhibits the prokaryotic ribosome 3.4 times poorer than **3** (IC_{50}^{Pro} values of 1.02 and 0.3 μM, respectively) is subsequently significantly less toxic than compound **3**. In addition, it is of note that the observed biological data reveal that the same modification of the 5″-NH_2 in **1** and **2** (conversion to 5″-NH−CH_2CH_2OH) has the opposite effect in terms of toxicity; in **1** → **3**, the toxicity increases by 4.6-fold (BHK) and 6.4-fold (HEK293-FT), while in **2** → **6** the toxicity decreases by 3.0-fold (BHK) and 2.4-fold (HEK293-FT). The observed increased toxicity can be explained particularly based on the 2.8-fold stronger inhibition of the prokaryotic ribosome in **3** vs **1**.

But the observed decreased toxicity can be explained mainly by 6.5-fold poorer inhibition of the eukaryotic ribosome in **6** vs **2**. To decipher the observed trends in the biological activity of **1**, **2**, **3**, and **6**, we performed molecular dynamics (MD) simulations of their binding in the A site in the eukaryotic ribosome. We prepared the 35 Å spherical model of the ribosome based on the crystal structure of 80S yeast ribosome (PDB code: 5DNV[26]) (Figure S1). Using Hamiltonian replica-exchange molecular dynamics (H-REMD)[27] followed by microsecond-long classical MD (see Theoretical Section in the Supporting Information (SI)), we performed an extensive conformational sampling of the aminoglycosides to determine their optimal binding modes and structural properties in the ribosomal A site.

We also calculated relative binding free energies of the aminoglycosides using Thermodynamic Integration (TI)[28] (see Theoretical Section in the SI) to assess their relationship with IC_{50}^{Euk} and readthrough activity.

We found that for all of the compounds the conformation of rings I and II corresponds to the canonical binding mode of aminoglycosides derived from paromamine, in which ring I is stacked to A1491 and interacts with A1492 and G1408 (Figure S2A) while ring II anchors the aminoglycoside at the binding site via the interactions with A1493, G1494, and U1495 (using the nucleotide numbering of *E. coli*)[26] (Figure S2B). However, the conformation of ring III and its interactions with A site residues (1406−1409) are different among the investigated compounds (Figures 4 and S2C).

For compounds **1**, **3**, and **6**, a ribose scaffold of ring III adopts an orientation in which 2″ and 3″ hydroxyls interact with the amine of C1407 and the phosphate of U1406, respectively (Figure 4A, C, D). This in turn allows the protonated amine at 5″ to form a hydrogen bond with the carbonyl group of G1408. Compounds **3** and **6** additionally create a hydrogen bond with the amine of C1409 via the side-chain hydroxyl.

Interestingly, compound **2** acquires a rotated geometry of ring III, in which only 3″−OH maintains an interaction with U1406 while 2″−OH is exposed to the solvent (Figure 4B). However, the resulting loss in stabilization is greatly compensated by a triple hydrogen bonding formed between 5″-ammonium and the carbonyl and imidazole groups of G1408 and the amine of C1407. The large structural difference in binding mode between compounds **1**, **3**, **6**, and **2** is reflected in their relative binding free energies. Compound **2** is about 1.85 kcal/mol more potent binder than compound **1** (Table S1), which correlates well with its 7-fold lower IC_{50}^{Euk} (Table 1). The differences in binding free energy are below 0.15 kcal/mol for compounds **1**, **3**, and **6** (Table S1), which correlates with their similar IC_{50}^{Euk} (Table 1).

It may be conjectured that the highest readthrough activity of compound **2** is primarily attributed to the strong binding affinity for the decoding site, which translates into a higher number of occupied ribosomes over time and thus a higher probability of the PTC readthrough. Given that compounds **1**, **3**, and **6** show similar binding affinities for the eukaryotic ribosome, we were intrigued as to what lies behind their diverse readthrough activities and whether it is somehow determined by the way these aminoglycosides bind to the A site.

Extensive classical MD simulations showed that the investigated aminoglycosides exhibit different conformational dynamics of ring III, which is mainly determined by the stability of the 5″-amine interaction with G1408. Compounds **2** and **6** bearing a methyl group at the 5″ position maintained a stable conformation of ring III as indicated by low atomic fluctuations (0.454 $Å^2$ for **2** and 0.630 $Å^2$ for **6**) (Figure S3). The interaction with G1408 via 5″-amine was remarkably durable, as it formed for about 93% and 82% of the simulation time for compound **2** and **6**, respectively (Figure S4A,B). Compound **6** also demonstrated a stable hydrogen bond with C1409 via the side-chain hydroxyl, which persisted for 94% of the simulation time.

In contrast, the ring III conformation of compounds **1** and **3** was more mobile as reflected in higher atomic fluctuations (0.582 $Å^2$ for **1** and 1.617 $Å^2$ for **3**) (Figure S3). The interaction between 5″-amine and G1408 was more labile, as it was maintained for only about 39% and 25% of the simulation time for compounds **1** and **3**, respectively (Figure S4C,D). For the remaining time, 5″-amine of compounds **1** and **3** was exposed to water, while the side chain in compound **3** visited several conformations in which it interacted with U1410, A1490, and A1491 residues.

The readthrough activity of aminoglycosides containing 6′-OH in ring I has been suggested to result from functional mispairing of near-cognate tRNA with a premature stop codon,

https://doi.org/10.1021/acsmedchemlett.3c00089
ACS Med. Chem. Lett. 2023, 14, 794−801

when bound to the decoding site in eukaryotic ribosome.[20,29] In addition, it has been proposed that recognition of the stop codon by the peptide release factor, enabling completion of the translation process, requires a specific structural rearrangement of the A site.[30] In light of our results, we hypothesize that aminoglycosides with increased conformational stability in the binding site may kinetically trap the rRNA in a geometry that favors near-cognate tRNA binding to the stop codon over the release factor protein. Conversely, compounds with lower kinetic stability may be more susceptible to destabilization of the binding site by the release factor protein, so that the stop codon is recognized correctly and the translation process is terminated. To verify that hypothesis, large-scale MD simulations of the eukaryotic ribosome with tRNA and release factor competing for mRNA are currently in progress.

In summary, in efforts to balance the readthrough activity and toxicity of the newly designed aminoglycosides as efficient PTC suppressors, we hypothesized that by installing an ethyl alcohol moiety on the primary 5″-amine of **1** and **2**, we may impact the basicity of the 5″-amine and subsequently the anticipated toxicity of the resulted structures. These efforts lead to the discovery of the new lead structure, compound **6**, exhibiting significant readthrough activity and considerably lower toxicity than the previous lead compound **2**. The improved safety of **6** boosts its therapeutic potential for treatment of a wide range of severe genetic diseases caused by PTCs. Further tests of **6** in *ex vivo* models of various genetic diseases along with its comparative nephrotoxicity and ototoxicity tests are currently underway.

■ ASSOCIATED CONTENT

Supporting Information

The Supporting Information is available free of charge at https://pubs.acs.org/doi/10.1021/acsmedchemlett.3c00089.

Biochemical assays, synthetic procedures, copies of NMR spectra of all the new products **3**−**7**, computational methods, and simulation data (PDF)

■ AUTHOR INFORMATION

Corresponding Author

Timor Baasov − *The Edith and Joseph Fischer Enzyme Inhibitors Laboratory, Schulich Faculty of Chemistry, Technion - Israel Institute of Technology, Haifa 3200003, Israel*; orcid.org/0000-0002-1427-2619; Phone: +972-4-829-2590; Email: chtimor@technion.ac.il

Authors

Sandip Guchhait − *The Edith and Joseph Fischer Enzyme Inhibitors Laboratory, Schulich Faculty of Chemistry, Technion - Israel Institute of Technology, Haifa 3200003, Israel*

Alina Khononov − *The Edith and Joseph Fischer Enzyme Inhibitors Laboratory, Schulich Faculty of Chemistry, Technion - Israel Institute of Technology, Haifa 3200003, Israel*

Tomasz Pieńko − *The Edith and Joseph Fischer Enzyme Inhibitors Laboratory, Schulich Faculty of Chemistry, Technion - Israel Institute of Technology, Haifa 3200003, Israel*

Valery Belakhov − *The Edith and Joseph Fischer Enzyme Inhibitors Laboratory, Schulich Faculty of Chemistry, Technion - Israel Institute of Technology, Haifa 3200003, Israel*

Complete contact information is available at: https://pubs.acs.org/10.1021/acsmedchemlett.3c00089

Author Contributions

†S.G., A.K., and T.P. contributed equally. The manuscript was written through contributions of all authors. All authors have given approval to the final version of the manuscript.

Funding

This work was supported by Eloxx Pharmaceutical LTD Research Fund (Grant No. 2030646).

Notes

The authors declare the following competing financial interest(s): T.B. declares that the compounds 1-7 discussed in this publication are subject to license agreement granted to a commercial third party.

■ ACKNOWLEDGMENTS

S.G. acknowledges the Silvia Noiman postdoctoral research fund established by Eloxx Pharmaceutical Ltd. V.B. acknowledges the Ministry of Science and Technology, Israel (Kamea Program). The MD simulations were performed in Technion - Israel Institute of Technology and Interdisciplinary Centre for Mathematical and Computational Modelling of the University of Warsaw, Poland (GR83-22).

■ ABBREVIATIONS

PTC, premature termination codon; CF, cystic fibrosis; USH, Usher syndrome

■ REFERENCES

(1) Keeling, K. M.; Xue, X.; Gunn, G.; Bedwell, D. M. Therapeutics Based on Stop Codon Readthrough. *Annu. Rev. Genomics Hum. Genet.* **2014**, *15*, 371−394.

(2) Keeling, K. M.; Bedwell, D. M. Pharmacological Suppression of Premature Stop Mutations That Cause Genetic Diseases. *Curr. Pharmacogenomics* **2005**, *3* (4), 259−269.

(3) Kellermayer, R. Translational Readthrough Induction of Pathogenic Nonsense Mutations. *Eur. J. Med. Genet* **2006**, *49* (6), 445−450.

(4) Burke, J. F.; Mogg, A. E. Suppression of a Nonsense Mutation in Mammalian Cells in Vivo by the Aminoglycoside Antibiotics G-418 and Paromomycin. *Nucleic Acids Res.* **1985**, *13* (17), 6265−6272.

(5) Kaufman, R. J. Correction of Genetic Disease by Making Sense from Nonsense. *J. Clin. Invest.* **1999**, *104* (4), 367−368.

(6) Kerem, E. Pharmacologic Therapy for Stop Mutations: How Much CFTR Activity Is Enough? *Curr. Opin. Pulm. Med.* **2004**, *10* (6), 547−552.

(7) Nudelman, I.; Rebibo-Sabbah, A.; Shallom-Shezifi, D.; Hainrichson, M.; Stahl, I.; Ben-Yosef, T.; Baasov, T. Redesign of Aminoglycosides for Treatment of Human Genetic Diseases Caused by Premature Stop Mutations. *Bioorg. Med. Chem. Lett.* **2006**, *16* (24), 6310−6315.

(8) Hainrichson, M.; Nudelman, I.; Baasov, T. Designer Aminoglycosides: The Race to Develop Improved Antibiotics and Compounds for the Treatment of Human Genetic Diseases. *Org. Biomol Chem.* **2008**, *6* (2), 227−239.

(9) Nudelman, I.; Rebibo-Sabbah, A.; Cherniavsky, M.; Belakhov, V.; Hainrichson, M.; Chen, F.; Schacht, J.; Pilch, D. S.; Ben-Yosef, T.; Baasov, T. Development of Novel Aminoglycoside (NB54) with Reduced Toxicity and Enhanced Suppression of Disease-Causing Premature Stop Mutations. *J. Med. Chem.* **2009**, *52* (9), 2836−2845.

(10) Nudelman, I.; Glikin, D.; Smolkin, B.; Hainrichson, M.; Belakhov, V.; Baasov, T. Repairing Faulty Genes by Aminoglycosides:

Development of New Derivatives of Geneticin (G418) with Enhanced Suppression of Diseases-Causing Nonsense Mutations. *Bioorg. Med. Chem.* **2010**, *18*, 3735−3746.
(11) Kandasamy, J.; Atia-Glikin, D.; Belakhov, V.; Baasov, T. Repairing Faulty Genes by Aminoglycosides: Identification of New Pharmacophore with Enhanced Suppression of Disease-Causing Nonsense Mutations. *Medchemcomm* **2011**, *2* (3), 165−171.
(12) Kandasamy, J.; Atia-Glikin, D.; Shulman, E.; Shapira, K.; Shavit, M.; Belakhov, V.; Baasov, T. Increased Selectivity toward Cytoplasmic versus Mitochondrial Ribosome Confers Improved Efficiency of Synthetic Aminoglycosides in Fixing Damaged Genes: A Strategy for Treatment of Genetic Diseases Caused by Nonsense Mutations. *J. Med. Chem.* **2012**, *55*, 10630−10643.
(13) Brasell, E. J.; Chu, L. L.; Akpa, M. M.; Eshkar-Oren, I.; Alroy, I.; Corsini, R.; Gilfix, B. M.; Yamanaka, Y.; Huertas, P.; Goodyer, P. The Novel Aminoglycoside, ELX-02, Permits CTNSW138X Translational Read-through and Restores Lysosomal Cystine Efflux in Cystinosis. *PLoS One* **2019**, *14* (12), e0223954.
(14) Shulman, E.; Belakhov, V.; Wei, G.; Kendall, A.; Meyron-Holtz, E. G.; Ben-Shachar, D.; Schacht, J.; Baasov, T. Designer Aminoglycosides That Selectively Inhibit Cytoplasmic Rather than Mitochondrial Ribosomes Show Decreased Ototoxicity a Strategy for the Treatment of Genetic Diseases. *J. Biol. Chem.* **2014**, *289* (4), 2318−2330.
(15) Baiazitov, R. Y.; Friesen, W.; Johnson, B.; Mollin, A.; Sheedy, J.; Sierra, J.; Weetall, M.; Branstrom, A.; Welch, E.; Moon, Y. C. Chemical Modifications of G418 (Geneticin): Synthesis of Novel Readthrough Aminoglycosides Results in an Improved in Vitro Safety Window but No Improvements in Vivo. *Carbohydr. Res.* **2020**, *495*, 108058−108064.
(16) Manuvakhova, M.; Keeling, K.; Bedwell, D. M. Aminoglycoside Antibiotics Mediate Context-Dependent Suppression of Termination Codons in a Mammalian Translation System. *Rna* **2000**, *6* (7), 1044−1055.
(17) Chernikov, V. G.; Terekhov, S. M.; Krokhina, T. B.; Shishkin, S. S.; Smirnova, T. D.; Kalashnikova, E. A.; Adnoral, N. V.; Rebrov, L. B.; Denisov-Nikol'skii, Y. I.; Bykov, V. A. Comparison of Cytotoxicity of Aminoglycoside Antibiotics Using a Panel Cellular Biotest System. *Bull. Exp. Biol. Med.* **2003**, *135* (1), 103−105.
(18) Popadynec, M.; Baradaran-Heravi, A.; Alford, B.; Cameron, S. A.; Clinch, K.; Mason, J. M.; Rendle, P. M.; Zubkova, O. V.; Gan, Z.; Liu, H.; Rebollo, O.; Whitfield, D. M.; Yan, F.; Roberge, M.; Powell, D. A. Reducing the Toxicity of Designer Aminoglycosides as Nonsense Mutation Readthrough Agents for Therapeutic Targets. *ACS Med. Chem. Lett.* **2021**, *12* (9), 1486−1492.
(19) Sabbavarapu, N. M.; Shavit, M.; Degani, Y.; Smolkin, B.; Belakhov, V.; Baasov, T. Design of Novel Aminoglycoside Derivatives with Enhanced Suppression of Diseases-Causing Nonsense Mutations. *ACS Med. Chem. Lett.* **2016**, *7* (4), 418−423.
(20) Shalev, M.; Baasov, T. When Proteins Start to Make Sense: Fine-Tuning of Aminoglycosides for PTC Suppression Therapy. *Medchemcomm* **2014**, *5* (8), 1092−1105.
(21) Shalev, M.; Rozenberg, H.; Smolkin, B.; Nasereddin, A.; Kopelyanskiy, D.; Belakhov, V.; Schrepfer, T.; Schacht, J.; Jaffe, C. L.; Adir, N.; Baasov, T. Structural Basis for Selective Targeting of Leishmanial Ribosomes: Aminoglycoside Derivatives as Promising Therapeutics. *Nucleic Acids Res.* **2015**, *43* (17), 8601−8613.
(22) Chen, L.; Hainrichson, M.; Bourdetsky, D.; Mor, A.; Yaron, S.; Baasov, T. Structure-Toxicity Relationship of Aminoglycosides: Correlation of 2'-Amine Basicity with Acute Toxicity in Pseudo-Disaccharide Scaffolds. *Bioorg. Med. Chem.* **2008**, *16* (19), 8940−8951.
(23) Fujisawa, K.-I.; Hoshiya, T.; Kawaguchi, H. Aminoglycoside Antibitotics. VII Acute Toxicity Of Aminoglycoside Antibitotics. *J. Antibitoics* **1974**, *27* (9), 677−681.
(24) Shitara, T.; Kobayashi, Y.; Tsuchiya, T.; Umezawa, S. Synthesis of 5-Deoxy-5-Fluoro and 5-Deoxy-5,5-Difluoro Derivatives of Kanamycin-B and Its Analogs - Study on Structure Toxicity Relationships. *Carbohydr. Res.* **1992**, *232* (2), 273−290.
(25) Shitara, T.; Umemura, E.; Tsuchiya, T.; Matsuno, T. Synthesis of 5-Deoxy-5-Epifluoro Derivatives of Arbekacin, Amikacin, and 1-N-[(S)-4-Amino-2-Hydroxybutanoyl]Tobramycin (Study on Structure-Toxicity Relationships). *Carbohydr. Res.* **1995**, *276* (1), 75−89.
(26) Prokhorova, I.; Altman, R. B.; Djumagulov, M.; Shrestha, J. P.; Urzhumtsev, A.; Ferguson, A.; Chang, C. W. T.; Yusupov, M.; Blanchard, S. C.; Yusupova, G. Aminoglycoside Interactions and Impacts on the Eukaryotic Ribosome. *Proc. Natl. Acad. Sci. U. S. A.* **2017**, *114* (51), 10899−10908.
(27) Roe, D. R.; Bergonzo, C.; Cheatham, T. E. I. I. I. Evaluation of Enhanced Sampling Provided by Accelerated Molecular Dynamics with Hamiltonian Replica Exchange Methods. *J. Phys. Chem. B* **2014**, *118* (13), 3543−3552.
(28) Lee, T.-S.; Allen, B. K.; Giese, T. J.; Guo, Z.; Li, P.; Lin, C.; McGee, T. D. J.; Pearlman, D. A.; Radak, B. K.; Tao, Y.; Tsai, H.-C.; Xu, H.; Sherman, W.; York, D. M. Alchemical Binding Free Energy Calculations in AMBER20: Advances and Best Practices for Drug Discovery. *J. Chem. Inf. Model.* **2020**, *60* (11), 5595−5623.
(29) Ng, M. Y.; Li, H.; Ghelfi, M. D.; Goldman, Y. E.; Cooperman, B. S. Ataluren and Aminoglycosides Stimulate Read-through of Nonsense Codons by Orthogonal Mechanisms. *Proc. Natl. Acad. Sci. U. S. A.* **2021**, *118* (2), e2020599118.
(30) Youngman, E. M.; He, S. L.; Nikstad, L. J.; Green, R. Stop Codon Recognition by Release Factors Induces Structural Rearrangement of the Ribosomal Decoding Center That Is Productive for Peptide Release. *Mol. Cell* **2007**, *28* (4), 533−543.

https://doi.org/10.1021/acsmedchemlett.3c00089
ACS Med. Chem. Lett. 2023, 14, 794−801